Comprehensive Clinical Evaluation of Femoroacetabular Impingement: Part 3, Magnetic Resonance Imaging

Andrew G. Geeslin, M.D., Matthew G. Geeslin, M.D., M.S., Jorge Chahla, M.D., Ph.D., Sandeep Mannava, M.D., Ph.D., Salvatore Frangiamore, M.D., M.S., and Marc J. Philippon, M.D.

Abstract: Radiologic imaging is an essential supplement to the physical examination in the evaluation of a patient with femoroacetabular impingement. Plain radiographs are the initial modality of choice for the evaluation of bony anatomy and pathology. Magnetic resonance imaging supplements the physical examination and standard radiographs by enabling qualitative and quantitative evaluation of both articular cartilage and soft tissues about the hip. Magnetic resonance imaging also provides improved 3-dimensional characterization of the bony anatomy owing to the multiplanar nature of this technique. This article describes a comprehensive approach to interpretation of magnetic resonance examination of the hip.

Imaging evaluation of the hip supplements a thorough physical examination in patients with hip pathology. Plain radiographs allow identification of bony pathology such as classic femoroacetabular impingement (FAI) findings including cam deformities, pincer lesions, and anterior inferior iliac subspine impingement. Radiographs also allow for objective evaluation of neck-shaft angle abnormalities, acetabular morphology, femoral head asphericity, avascular necrosis, traumatic injury, joint space narrowing, and subchondral cysts. Whereas magnetic resonance imaging (MRI) also facilitates characterization of these bony lesions, it is uniquely capable of evaluating the labrum, cartilage, ligamentum teres, synovial tissue, capsule, and adjacent muscles and tendons.

It is important to note that a 25-fold increase in hip arthroscopy volume between 2006 and 2013 was reported.[1] As hip arthroscopy continues to grow as a discipline, the further incorporation of sophisticated imaging into clinical practice is expected. An orthopaedic surgeon should be adept at selecting the appropriate imaging modality to evaluate hip pathology, as well as interpreting the radiographic findings. However, partnership with a designated musculoskeletal radiologist is paramount, especially when reviewing advanced MRI techniques. This article is part 3 of a 3-part series; part 1 addressed the physical examination,[2] and part 2 addressed interpretation of plain radiographs.[3] The purpose of this Technical Note is to describe a comprehensive approach to interpretation of hip MRI for the orthopaedic surgeon. A description of an example MRI protocol is included, along with a discussion of the optimal sequences and planes for identifying key pathology and quantifying bony morphology.

MRI Technique

Most institutions have a standard set of imaging planes and sequences for each imaging modality and indication, and the referring clinician should have a

From the Steadman Philippon Research Institute (A.G.G., J.C., S.M., S.F., M.J.P.), Vail, Colorado; University of Virginia School of Medicine (M.G.G.), Charlottesville, Virginia; and The Steadman Clinic (M.J.P.), Vail, Colorado, U.S.A.

The authors report the following potential conflict of interest or source of funding: S.M. receives American Board of Medical Specialties (ABMS)-American Board of Orthopaedic Surgeons (ABOS) Visiting Scholars Grant; he was also awarded with US Patent 08926626. M.J.P. receives support from ISHA, Smith & Nephew, MIS, MJP Innovations, LLC, Ossur, Siemens, Vail Valley Medical Center, Arthrosurface, DonJoy, Slack, Elsevier, and Linvatec. Full ICMJE author disclosure forms are available for this article online, as supplementary material.

Received March 29, 2017; accepted June 29, 2017.

Address correspondence to Marc J. Philippon, M.D., Steadman Philippon Research Institute, The Steadman Clinic, 181 W Meadow Dr, Ste 400, Vail, CO 81657, U.S.A. E-mail: drphilippon@sprivail.org

2212-6287/17425

http://dx.doi.org/10.1016/j.eats.2017.06.062

Table 1. Commonly Obtained Hip MRI Planes and Sequences

Technique	Imaging Plane	Sequence
1	Axial	T2 TSE
2	Axial oblique	PD FS
3	Axial (knee)*	T1 TSE
4	Sagittal	PD TSE FS
5	Sagittal	PD
6	Sagittal	T2 mapping
7	Coronal	PD TSE
8	Coronal	PD TSE FS

FS, fat suppressed; MRI, magnetic resonance imaging; PD, proton density; TSE, turbo spin echo.

* Axial scout images are obtained at the knee to allow measurement of femoral neck version.

familiarity with the protocols. Specifically, hip MRI protocols comprise several imaging planes including an oblique plane along the femoral neck (to measure the alpha angle), as well as standard coronal, sagittal, and axial planes. Certain tissue weightings including T1, T2, and proton density (PD) may be obtained, and compositional cartilage imaging techniques may be performed. Often, the contralateral hip is included in the coronal series to allow comparison of marrow characteristics.

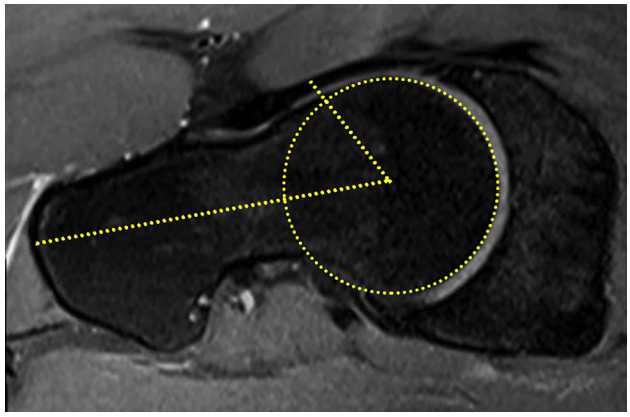

Fig 2. Measurement of the alpha angle allows quantification of the size of a cam deformity due to femoral head-neck offset abnormality. The technique for measurement of the alpha angle is shown in this right hip axial oblique proton density fat-suppressed magnetic resonance image. A best-fit circle is placed at the femoral head and preferentially aligned with the anterosuperior region. A second best-fit circle can be placed at the narrowest aspect of the femoral neck to allow localization of the neck axis. An angle is then drawn between the center of the femoral neck, the center of the femoral head (i.e., the apex of the angle), and the location where the femoral head extends beyond the boundary of the best-fit circle (i.e., becomes out of round).

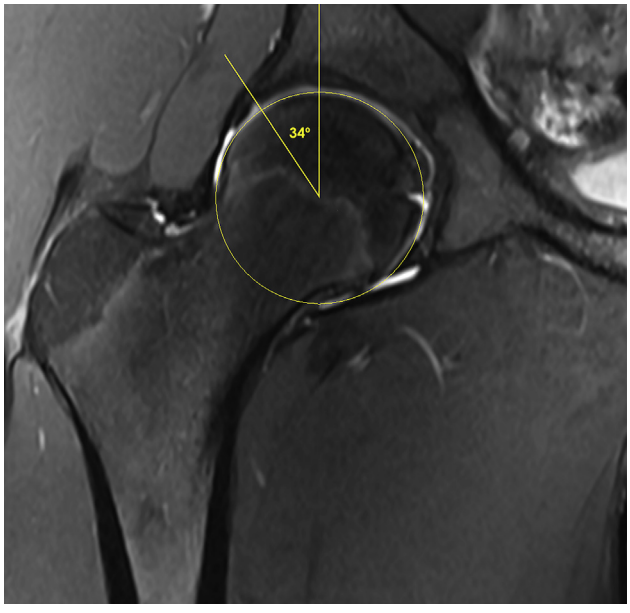

Fig 1. The lateral center-edge angle (LCEA) quantifies the amount of lateral overhang of the acetabulum. Measurement of the LCEA is shown in this right hip coronal proton density turbo spin echo fat-suppressed magnetic resonance image. An angle is made between the longitudinal pelvic axis, the center of the circle (the apex), and the lateral aspect of the acetabulum. The reported normal range is 25° to 40°, less than 20° is considered dysplastic, 20° to 25° is considered borderline dysplastic, and greater than 40° may be associated with a pincer lesion. The LCEA in this patient is 34° and considered to be within the normal range.

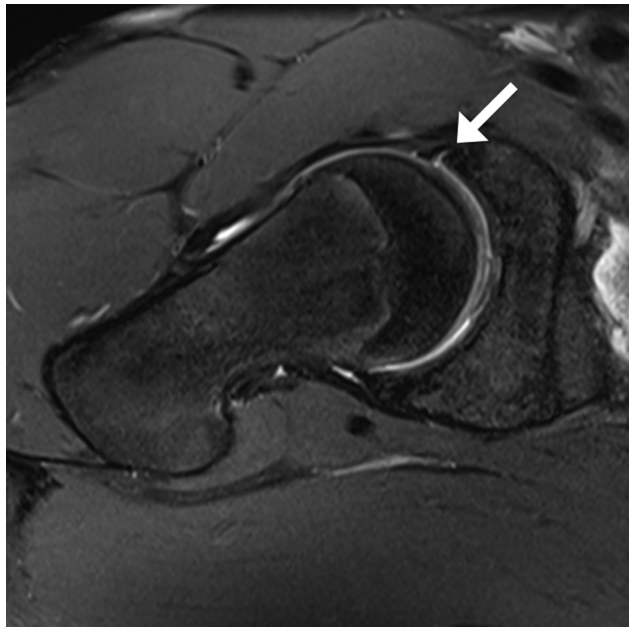

Fig 3. Fluid-sensitive sequences with axial oblique sections are optimal for identification of labral tears, although coronal sections may also be used. An anterosuperior labral tear (arrow) is shown in this right hip axial oblique proton density (PD) fat-suppressed (FS) magnetic resonance image. To better understand the 3-dimensional pattern of the tear, multiple imaging planes and sequences should be evaluated, including coronal PD turbo spin echo FS, axial T2 turbo spin echo, and axial oblique PD FS.

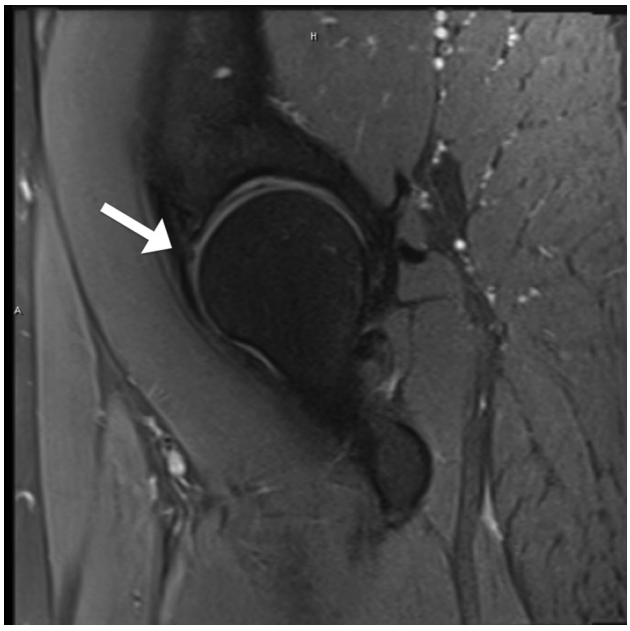

Fig 4. After arthroscopic labral debridement, symptoms of hip microinstability may develop in patients and labral deficiency may be identified on magnetic resonance imaging. Labral deficiency (arrow) is shown in this right hip sagittal proton density fat-suppressed magnetic resonance image in a patient referred for evaluation after a prior hip arthroscopy with labral debridement.

Some surgeons and radiologists request the injection of intra-articular contrast for more detailed evaluation of the labrum and cartilage.[4] However, most historical studies comparing hip MRI with and without intra-articular contrast were performed on 1.5-T platforms and may not be comparable to optimized, high-resolution, nonarthrographic 3-T MRI.[4] A recent study in patients with clinically suspected FAI reported that nonarthrographic 3-T MRI was highly accurate for evaluating the labrum and cartilage.[5] When combined with clinical history, physical examination, and plain radiography, high-resolution 3-T MRI allows avoidance of the need for intra-articular contrast. A standardized nonarthrographic hip MRI protocol is outlined in Table 1.[6]

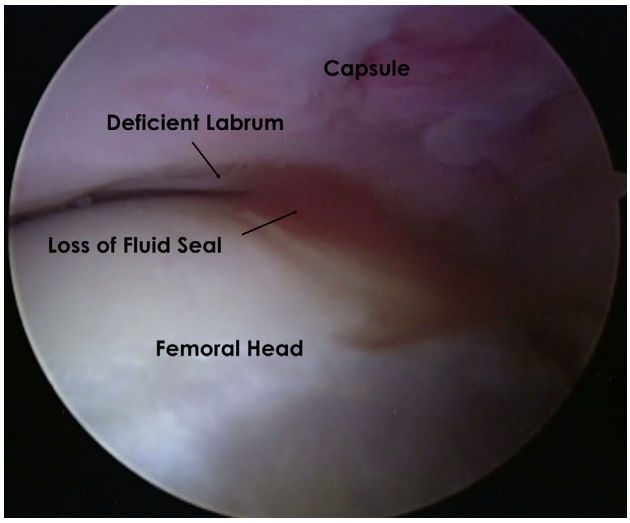

Fig 5. Capsulolabral adhesions may develop in patients with a prior labral tear and may present with microinstability due to loss of the normal labral suction seal. An arthroscopic image in a patient's left hip that underwent a prior labral repair (as viewed from the midanterior portal) shows capsulolabral adhesions. This patient underwent insertion of a capsulolabral spacer to restore the normal capsulolabral interval.

Table 2. Compositional Assessment of Articular Cartilage

MRI Technique	Molecular Component Assessed
T2 mapping	Water, collagen
T2* mapping	Water, collagen
T1ρ imaging	Collagen, GAGs
dGEMRIC	GAGs
Diffusion-weighted imaging	Collagen, GAGs

dGEMRIC, delayed gadolinium-enhanced magnetic resonance imaging of cartilage; GAGs, glycosaminoglycans; MRI, magnetic resonance imaging.

Comprehensive Interpretation of Hip MRI

Bone Morphologic Characteristics

MRI is optimized for soft-tissue characterization, and detailed evaluation of cortical bone is limited because of low relative proton density. Despite this limitation, cortical bone is sufficiently imaged on MRI and does not expose the patient to ionizing radiation, and quantitative analysis of bony morphology is allowed. However, there has been a trend toward use of computed tomography imaging to assist with surgical planning for FAI because of improved cortical bone imaging.[7] Although computed tomography may be optimized for cortical bone imaging, quantitative analysis of bony morphology is feasible on MRI.

Acetabular morphology is quantitatively described by measurement of the amount of femoral head coverage using the lateral center-edge angle.[8] By use of the coronal sequences, a best-fit circle is drawn to identify the center of the femoral head (Fig 1). An angle is made between the longitudinal pelvic axis, the center of the circle (the apex), and the lateral aspect of the acetabulum. The normal range is 25° to 40°, less than 20° is considered dysplastic, 20° to 25° is considered borderline dysplastic, and greater than 40° may be associated with a pincer lesion.[8]

Femoral head asphericity is quantified with the use of the alpha angle, as described by Notzli et al.,[9] and is performed on the T2 axial oblique series (Fig 2). The alpha angle allows quantitative characterization of the deformity associated with cam-type FAI. A best-fit circle is placed at the femoral head and preferentially aligned with the anterosuperior region. A second best-fit circle is placed at the narrowest aspect of the femoral neck to

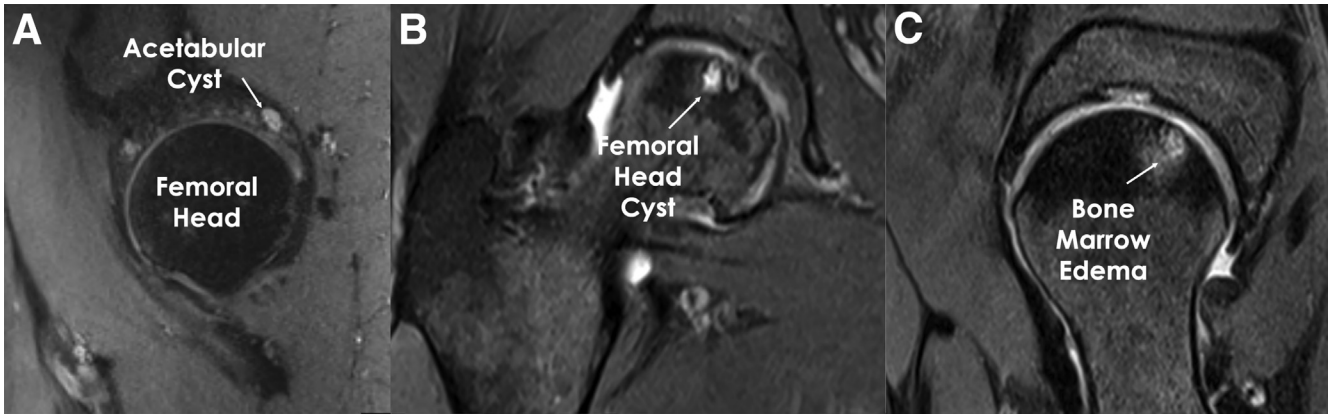

Fig 6. Fluid-sensitive magnetic resonance (MR) imaging sequences are optimal for identification of subchondral cysts and bony edema. (A) An acetabular subchondral cyst with overlying chondromalacia is shown in this right hip sagittal proton density (PD) fat-suppressed (FS) MR image. (B) A femoral head subchondral cyst with overlying chondromalacia is shown in this right hip coronal PD turbo spin echo FS MR image. (C) Bone marrow edema in the femoral head with overlying chondromalacia is shown in this right hip axial oblique PD FS MR image.

allow localization of the neck axis. An angle is then drawn between the center of the femoral neck, the center of the femoral head (i.e., the apex of the angle), and the location where the femoral head extends beyond the boundary of the best-fit circle (i.e., "becomes out of round").

Notzli et al.[9] reported that the mean alpha angle was 42° in asymptomatic control subjects and 74° in the symptomatic group; greater than 50° was considered large. Although the cutoff for a "normal" offset is debated, an alpha angle greater than 50° has been characterized as abnormal.[10-12] However, a higher threshold has also been suggested.[13,14] Nonetheless, it is important to consider that an abnormal femoral head-neck offset, characterized by an increased alpha angle, is a 3-dimensional (3D) anatomic entity, and variable measurements may be obtained in the same patient with different imaging planes and by different reviewers.[14]

Femoral neck version is measured by referencing the posterior condylar axis on an axial scout image of the distal femur.[15] It has been suggested that femoral neck version may have implications for treatment of iliopsoas pathology.

Fibrocystic changes, also known as impingement cysts, may be identified on both radiographs and MRI at the femoral head-neck junction.[16] These lesions are typically located at the anterosuperior femoral neck in the region of impingement; at the time of surgery, they are often included in the osteochondroplasty.[17] Large cysts may require grafting and can be filled with a biocomposite surgical screw.

Labrum

There is growing interest in the diagnosis and treatment of chondrolabral lesions, largely because of the increasing technical ability of treating FAI with hip arthroscopy. Despite advances in MRI hardware and

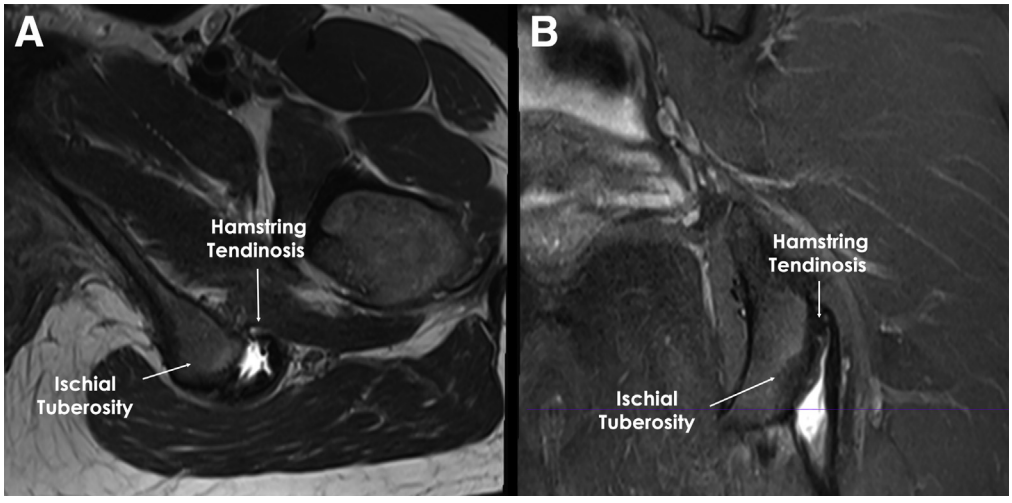

Fig 7. Tendinopathy is optimally identified on fluid-sensitive sequences and may be seen on coronal, sagittal, and axial sections. Left hip axial T2 turbo spin echo (A) and coronal proton density turbo spin echo fat-suppressed (B) magnetic resonance images show severe hamstring tendinosis in a professional female runner with femoroacetabular impingement.

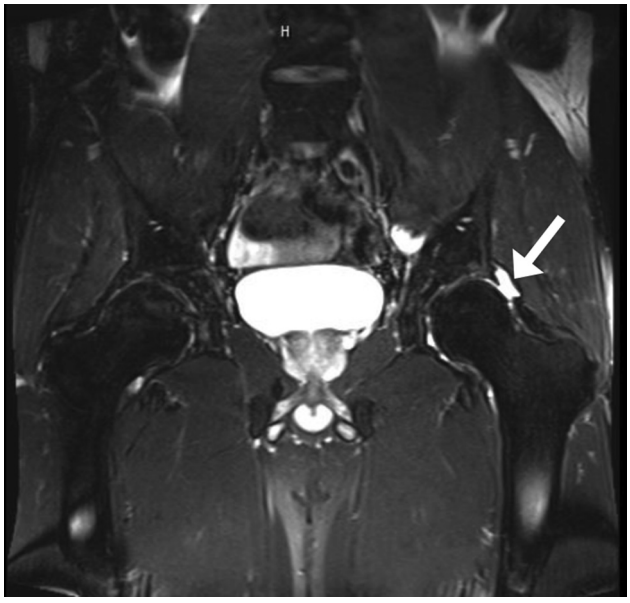

Fig 8. Capsular deficiency is associated with prior hip arthroscopy with unattempted or unsuccessful capsular closure. A full-pelvis coronal MR arthrogram shows left hip capsular deficiency (arrow) in a patient referred to us for treatment of residual symptoms after an arthroscopic hip procedure.

acquisition techniques that result in higher-resolution magnetic resonance (MR) images with improved signal-to-noise ratios, imaging of the articular cartilage and the labrum in the hip remains challenging. Labral tears and/or detachment may be identified on coronal, sagittal, and axial oblique images (Fig 3).

Although the most common location for labral pathology is the anterosuperior region, the labrum is evaluated circumferentially using several imaging sequences. Tear location is referenced using the clock face with the "psoas-u" located at the 3-o'clock position anteriorly.[18,19]

Pulse sequences with high in-plane resolution such as T1 fat-suppressed (FS), T2 FS, and 3D water excitation dual echo steady state (DESS) are most sensitive for labral evaluation.[4] Studies have reported a sensitivity and specificity of 80% to 97% and 85% to 100%, respectively, using T1 FS and T2 FS, with arthroscopy as the reference standard. Notably, 1 study using 3D DESS reported a sensitivity of 85% to 89% and a much wider specificity range of 50% to 100%.[4] Particularly, higher field strengths (3.0 T vs 1.5 T), small fields of view, and external small surface coils (as opposed to coils housed within the table) are nearly essential when imaging the labrum. Data regarding the use of high-resolution unenhanced 3-T MRI of the hip are limited, and further study comparing 3-T MRI and MR arthrography is a major requirement for validating the use of unenhanced 3-T MRI.

As the frequency of hip arthroscopic procedures increases,[1] so does the frequency of revision hip arthroscopy. Increased complexity is associated with these procedures, which may include labral reconstruction or labral augmentation for labral deficiency (Fig 4) or insertion of a capsulolabral spacer in the setting of capsulolabral adhesions (Fig 5).

Cartilage

The sensitivity of MRI and MR arthrography is limited in the morphologic evaluation of cartilage abnormalities of the hip, but specificity is typically high. This challenge gave rise to the use of compositional cartilage imaging.

Morphologic evaluation of cartilage refers to the assessment of its 3D structure, which is notably difficult with MRI because of the comparatively low-resolution imaging on a spheroid such as the femoral head. As in the case of labral evaluation, higher field strengths, small fields of view, and external small surface coils are vastly superior. The most well-studied sequence used for morphologic evaluation of cartilage is 3D DESS; however, T2 FS and PD (also called intermediate weighted) FS can also be used.[4]

Compositional assessment of cartilage is used to evaluate the molecular status of the fluid-filled collagen and proteoglycan network comprising hyaline cartilage. Post-acquisition processing then creates a color-coded map of the biochemical composition of the cartilage surface. Compositional techniques are being used more commonly in imaging articular surfaces,[20] but they require greater technical expertise and are not yet widely used. A list of cartilage mapping techniques that the orthopaedic surgeon may encounter, as well as the molecular components the techniques assess, are presented in Table 2. T2 mapping is routinely used for hip imaging at our institution.

Ho et al.[21] recently reported the results of a prospective study of T2 mapping in patients with FAI. Areas of damaged and healthy-appearing cartilage underwent intraoperative International Cartilage Repair Society grading followed by biopsy with subsequent histologic analysis. Increased T2 values were observed among damaged specimens compared with healthy specimens, with the greatest differences observed among specimens with mild degeneration, suggesting a role of T2 mapping for early detection of chondral lesions in the absence of gross morphologic changes.

Subchondral Changes

Subchondral cysts and bone marrow edema not identified on radiographs are readily identified on fluid-sensitive MRI (e.g., coronal PD turbo spin echo FS). It is important to scrutinize images for these findings because subchondral cysts are associated with full-thickness cartilage lesion as well as inferior outcomes

Table 3. Tumors of Pelvis and Proximal Femur

Pelvis (in order of decreasing incidence)
Miscellaneous benign lesions*
Chondrosarcoma
Ewing tumor
Osteosarcoma
Miscellaneous malignant lesions
Fibrosarcoma or malignant fibrous histiocytoma
Langerhans cell histiocytosis
Aneurysmal bone cyst
Fibrous dysplasia
Proximal femur (in order of decreasing incidence)
Fibrous dysplasia
Solitary bone cyst
Osteoid osteoma
Chondroblastoma
Giant cell tumor
Osteochondroma
Aneurysmal bone cyst
Langerhans cell histiocytosis

NOTE. Adapted from Bloem and Reidsma.[27]

*Osteomyelitis, osteochondroma, solitary bone cyst, giant cell tumor, osteoid osteoma, osteoblastoma, or lymphoma.

in age- and activity-matched control subjects.[22] Given the present challenges of morphologically evaluating a curved surface on MRI, subchondral cysts are a very useful secondary finding for cartilage injury. Soft-tissue (paralabral) cysts may be identified adjacent to a labral tear and can be a useful secondary sign of labral pathology.

Fluid-sensitive sequences are the most sensitive acquisitions for detecting cysts. The use of fat suppression provides greater contrast between fat-containing bone marrow and adjacent fluid (Fig 6).

Tendinopathy

Injury to extra-articular hip structures has been associated with intra-articular pathology (FAI) as a result of compensatory changes in excursion and muscle firing. Hamstring tendinosis has been associated with intra-articular hip pathology and impingement, most commonly in female patients with acetabular pincer morphology.[23] It may also be associated with or result from gluteus maximus dysfunction, leading to over-firing of the hamstring tendons (Fig 7). In addition, rectus femoris tendinosis has been described in association with FAI.[23] Iliopsoas pathology has also been implicated in association with FAI, although the preferred treatment is evolving.

The most sensitive sequence for diagnosing tendinosis is a fluid-sensitive acquisition with fat suppression, such as T2 FS. Viewing this sequence on axial and sagittal sections facilitates optimal evaluation of the major tendons crossing the hip, including the hamstrings, rectus femoris, iliopsoas, and gluteus medius and minimus (although the hip abductors are also well visualized on coronal sections).

Capsule

On the basis of basic science and clinical evidence, there has been a trend toward routine capsular closure in hip arthroscopy.[24] Not all hip arthroscopists close the capsule, and although a consensus on the topic is lacking, this may be a cause of iatrogenic instability. However, there is a relative paucity of literature on the topic of MRI evaluation of capsular integrity. It is our experience that MRI allows qualitative assessment of capsular integrity and assessment of capsular defects (Fig 8). Capsular reconstruction has been described for treatment of these defects.[25,26]

Benign and Malignant Tumors

Benign and malignant pathology may also be identified incidentally on MRI.[27] Table 3 lists the most common benign and malignant primary osseous tumors of the pelvis, as well as benign osseous lesions of the proximal femur, in order of decreasing frequency.

The standard MRI protocol for hip evaluation in the sports medicine population is unlikely to include short tau inversion recovery, diffusion-weighted, or post–intravenous contrast imaging sequences. Thus,

Table 4. Key Imaging Planes and Sequences for Identification and Evaluation of Common Hip Pathologic Findings in Patients With FAI

Pathology	Imaging Plane and Sequence	Finding
Labral tear	Axial T2 TSE Axial oblique PD FS Coronal PD TSE FS	Linear signal irregularity
Chondral lesion	Coronal PD TSE FS Sagittal T2 mapping	Discontinuity in articular surface
Cam deformity	Axial oblique PD FS	Increased alpha angle
Lateral overcoverage	Coronal PD TSE	Increased LCEA
Subchondral cysts or edema	Coronal PD TSE FS	Cyst formation
Tendinosis of hamstring, rectus, or iliopsoas	Sagittal PD TSE FS Axial T2 TSE	Increased fluid within tendon and/or partial tearing
Tendinosis of gluteus medius or minimus	Coronal PD TSE FS	Increased fluid within tendon and/or partial tearing

FAI, femoroacetabular impingement; FS, fat suppressed; LCEA, lateral center-edge angle; PD, proton density; TSE, turbo spin echo.

requiring the patient to return for further imaging will be necessary when the incidentally detected lesion cannot be definitively characterized as benign. Bloem and Reidsma[26] comprehensively described these lesions along with a pictorial review. The potential for soft-tissue tumors as well as malignant bone tumors underscores the importance of careful evaluation of all series images, as well as partnership with a musculoskeletal radiologist.

Comprehensive Evaluation

With the increased understanding of prearthritic and early-arthritic hip pathology, interpretation of hip MRI is an important skill for the orthopaedic surgeon. Video 1 reviews a comprehensive and systematic approach for hip MRI evaluation. This knowledge includes an understanding of each sequence used in a standard hip MR protocol, as well as the anatomic abnormality for which each acquisition is optimized (Table 4). An understanding of the clinical indication for hip MRI is also important. Taken together, these abilities help establish the surgeon's independence when reviewing a study while recommending the most appropriate diagnostic evaluation.

Discussion

This article details a systematic approach for interpretation of hip MRI for the orthopaedic surgeon. Combined with clinical evaluation and radiographic assessment, MRI improves the surgeon's ability to render a more specific diagnosis of hip pathology, which ultimately aids in preoperative patient counseling and surgical planning. Although MRI is optimized for soft-tissue evaluation, characterization of bony anatomy is also enhanced with this multiplanar technique.

The ability to thoroughly evaluate labral and chondral pathology continues to advance. Debate as to the necessity of joint distention with paramagnetic contrast agents for the morphologic evaluation of chondral and labral lesions is ongoing, and larger-scale studies are necessary to evaluate comparable sensitivity of MRI for labral pathology in the presence and absence of intra-articular contrast. Improved identification of chondral and labral pathology is supported by searching for secondary signs of injury such as osseous and soft-tissue cystic lesions, respectively. These findings are most sensitively identified on T2 FS sequences.

Incidentally imaged osseous lesions in the pelvis and proximal femur require constant vigilance when reviewing these studies. As discussed, when a definitive benign characterization cannot be obtained, further imaging and possibly tissue sampling with biopsy by the treating orthopaedic oncologist may be required. As imaging techniques continue to advance, improved familiarity by the orthopaedic surgeon, along with musculoskeletal radiologist partnership, will lead to improved care for patients with hip pathology.

References

1. Cvetanovich GL, Chalmers PN, Levy DM, et al. Hip arthroscopy surgical volume trends and 30-day postoperative complications. *Arthroscopy* 2016;32:1286-1292.
2. Frangiamore S, Mannava S, Geeslin AG, Cinque ME, Chahla J, Philippon MJ. Comprehensive evaluation of the hip: Part 1, physical examination. *Arthrosc Tech* 2017;6:e1993-e2001.
3. Mannava S, Geeslin AG, Frangiamore SJ, et al. Comprehensive clinical evaluation of femoroacetabular impingement: Part 2, plain radiography. *Arthrosc Tech* 2017;6:e2003-e2009.
4. Naraghi A, White LM. MRI of labral and chondral lesions of the hip. *AJR Am J Roentgenol* 2015;205:479-490.
5. Linda DD, Naraghi A, Murnaghan L, Whelan D, White LM. Accuracy of non-arthrographic 3T MR imaging in evaluation of intra-articular pathology of the hip in femoroacetabular impingement. *Skeletal Radiol* 2017;46:299-308.
6. Ho CP, Ommen ND, Bhatia S, et al. Predictive value of 3-T magnetic resonance imaging in diagnosing grade 3 and 4 chondral lesions in the hip. *Arthroscopy* 2016;32:1808-1813.
7. Milone MT, Bedi A, Poultsides L, et al. Novel CT-based three-dimensional software improves the characterization of cam morphology. *Clin Orthop Relat Res* 2013;471:2484-2491.
8. Wiberg G. Studies on dysplastic acetabula. *Acta Chir Scand* 1939;83:1-135.
9. Notzli HP, Wyss TF, Stoecklin CH, Schmid MR, Treiber K, Hodler J. The contour of the femoral head-neck junction as a predictor for the risk of anterior impingement. *J Bone Joint Surg Br* 2002;84:556-560.
10. Barton C, Salineros MJ, Rakhra KS, Beaule PE. Validity of the alpha angle measurement on plain radiographs in the evaluation of cam-type femoroacetabular impingement. *Clin Orthop Relat Res* 2011;469:464-469.
11. Tannast M, Siebenrock KA, Anderson SE. Femoroacetabular impingement: Radiographic diagnosis—What the radiologist should know. *AJR Am J Roentgenol* 2007;188:1540-1552.
12. Ross JR, Larson CM, Adeoye O, Kelly BT, Bedi A. Residual deformity is the most common reason for revision hip arthroscopy: A three-dimensional CT study. *Clin Orthop Relat Res* 2015;473:1388-1395.
13. Agten CA, Sutter R, Buck FM, Pfirrmann CW. Hip imaging in athletes: Sports imaging series. *Radiology* 2016;280:351-369.
14. Sutter R, Dietrich TJ, Zingg PO, Pfirrmann CW. How useful is the alpha angle for discriminating between symptomatic patients with cam-type femoroacetabular impingement and asymptomatic volunteers? *Radiology* 2012;264:514-521.
15. Ejnisman L, Philippon MJ, Lertwanich P, et al. Relationship between femoral anteversion and findings in hips with femoroacetabular impingement. *Orthopedics* 2013;36:e293-e300.

16. Leunig M, Beck M, Kalhor M, Kim YJ, Werlen S, Ganz R. Fibrocystic changes at anterosuperior femoral neck: Prevalence in hips with femoroacetabular impingement. *Radiology* 2005;236:237-246.
17. Leunig M, Mast NH, Impellizerri FM, Ganz R, Panaro C. Arthroscopic appearance and treatment of impingement cysts at femoral head-neck junction. *Arthroscopy* 2012;28:66-73.
18. Lee WA, Saroki AJ, Loken S, et al. Radiographic identification of arthroscopically relevant acetabular structures. *Am J Sports Med* 2016;44:67-73.
19. Philippon MJ, Michalski MP, Campbell KJ, et al. An anatomical study of the acetabulum with clinical applications to hip arthroscopy. *J Bone Joint Surg Am* 2014;96:1673-1682.
20. Surowiec RK, Lucas EP, Ho CP. Quantitative MRI in the evaluation of articular cartilage health: Reproducibility and variability with a focus on T2 mapping. *Knee Surg Sports Traumatol Arthrosc* 2014;22:1385-1395.
21. Ho CP, Surowiec RK, Frisbie DD, et al. Prospective in vivo comparison of damaged and healthy-appearing articular cartilage specimens in patients with femoroacetabular impingement: Comparison of T2 mapping, histologic endpoints, and arthroscopic grading. *Arthroscopy* 2016;32:1601-1611.
22. Krych AJ, King AH, Berardelli RL, Sousa PL, Levy BA. Is subchondral acetabular edema or cystic change on MRI a contraindication for hip arthroscopy in patients with femoroacetabular impingement? *Am J Sports Med* 2016;44:454-459.
23. Hammoud S, Bedi A, Voos JE, Mauro CS, Kelly BT. The recognition and evaluation of patterns of compensatory injury in patients with mechanical hip pain. *Sports Health* 2014;6:108-118.
24. Harris JD, Slikker W III, Gupta AK, McCormick FM, Nho SJ. Routine complete capsular closure during hip arthroscopy. *Arthrosc Tech* 2013;2:e89-e94.
25. Chahla J, Dean CS, Soares E, Mook WR, Philippon MJ. Hip capsular reconstruction using dermal allograft. *Arthrosc Tech* 2016;5:e365-e369.
26. Mei-Dan O, Garabekyan T, McConkey M, Pascual-Garrido C. Arthroscopic anterior capsular reconstruction of the hip for recurrent instability. *Arthrosc Tech* 2015;4:e711-e715.
27. Bloem JL, Reidsma II. Bone and soft tissue tumors of hip and pelvis. *Eur J Radiol* 2012;81:3793-3801.